Tracing the refractive index profile of a multiple-ring two-mode fiber by analyzing modal interference feedback

Jiali Zhang
School of Information Engineering and Guangdong Provincial Key Laboratory of Information Photonics Technology
Guangdong University of Technology
Guangzhou, China

Quandong Huang
School of Information Engineering and Guangdong Provincial Key Laboratory of Information Photonics Technology
Guangdong University of Technology
Guangzhou, China
E-mail: qdhuang@gdut.edu.cn

Lixi Zhong
School of Information Engineering and Guangdong Provincial Key Laboratory of Information Photonics Technology
Guangdong University of Technology
Guangzhou, China

Jianping Li
School of Information Engineering and Guangdong Provincial Key Laboratory of Information Photonics Technology
Guangdong University of Technology
Guangzhou, China

Yuwen Qin
School of Information Engineering and Guangdong Provincial Key Laboratory of Information Photonics Technology
Guangdong University of Technology
Guangzhou, China

Ou Xu
School of Information Engineering and Guangdong Provincial Key Laboratory of Information Photonics Technology
Guangdong University of Technology
Guangzhou, China
E-mail: xuou@gdut.edu.cn

***Abstract*—We present a methodology to trace the refractive index profile of a multiple-ring two-mode fiber by analyzing modal interference, serving for exploring specialized applications in the optical communication area.**

Keywords—few-mode fiber, modal interference, fiber modes

I. INTRODUCTION

Few-mode fiber (FMF) plays an important role in the area of large capacity optical transmission, optical fiber sensing, optical imaging, and signal processing [1]-[4]. FMF, which can provide several independent channels by the use of guide modes in a single optical fiber, has been explored to support several times of the transmission capacity comparing with a standard single-mode fiber (SMF) via the mode division multiplexing (MDM) technology [5]. In an MDM system, optical components, such as mode multiplexers [6], mode converters [7], and mode filters [8], are building blocks of the MDM transmission frame. However, the accurate parameters of an FMF are essential to be known to predict and analyze its behavior or characteristics. By knowing the detailed information of an unknown FMF, we can further develop the FMF to work as an all-fiber functional optical device [9].

In this paper, we propose a methodology to deduce the refractive index profile of a multiple-ring two-mode fiber (TMF). According to the experimental results, we reproduce the parameters of the multiple-ring TMF by using modal interference and finite element method (FEM)-based calculation. The approach can be developed to serve as in-line fiber quality qualification system, and offers key proofs of special fibers before they are utilized to develop as functional components.

II. METHODOLOGY AND OPERATION PRINCIPLE

There are many instruments that can test a special fiber by measuring the material compositions, profiles, and defects. However, the cost of the instruments is usually expensive. Here, we present a simple optical method to search the refractive index profile of a multiple-ring TMF by the use of modal interference and FEM-based calculation.

The modal interference is achieved via the lateral-offset aligning of a multiple-ring TMF with two SMFs. A schematic diagram of lateral-offset aligning is shown in Fig.1, where a segment of multiple-ring TMF is sandwiched between two SMFs with the same lateral-offset direction of the fiber ends.

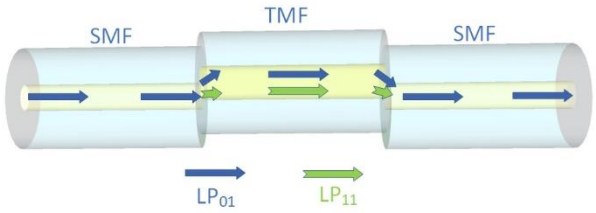

Fig. 1. Schematic diagram of the proposed lateral-offset aligning of a segment of multiple-ring TMF with two SMFs.

When broadband light is launched into the multiple-ring TMF from one end of SMF (labels as the first lateral-offset point), part of the LP_{01} mode is excited and converted to be the LP_{11} mode in the multiple-ring TMF. Then the LP_{01} mode and the LP_{11} mode arrive at the entrance of the other SMF (labels as the second lateral-offset point). Interference fringes that contribute by the LP_{01} mode and the LP_{11} mode occur. Output light intensity (I) against the wavelength can be express as

$$I = I_{LP_{01}} + I_{LP_{11}} - 2\sqrt{I_{LP_{01}} I_{LP_{11}}} cos\,(\Delta\varphi) \quad (1)$$

where $I_{LP_{01}}$ and $I_{LP_{11}}$ are the light intensities of the LP_{01} mode and the LP_{11} mode; $\Delta\varphi$ is the phase difference, which can be given as:

$$\Delta\varphi = \frac{2\pi}{\lambda}\Delta n_{eff} L \quad (2)$$

where λ is the central wavelength, Δn_{eff} is the effective refractive index difference of the LP_{01} mode and the LP_{11} mode, L is the length of the multiple-ring TMF. When the phase difference satisfies the condition of $\Delta\varphi=(2m+1)\pi$ with m of an integer, minimum output light intensity is achieved,

which is defined as resonant dip at specific wavelength. The wavelength range between the adjacent resonant dips is called free spectra range (FSR), which can be approximately expressed as

$$FSR = \frac{\lambda^2}{\Delta n_{eff} L} \tag{3}$$

It is obvious in Eq. (3) that the longer the length of multiple-ring TMF, the smaller FSR will be. As a result, more accurate effective index difference between the LP_{01} mode and the LP_{11} mode will be obtained with a longer multiple-ring TMF. By knowing the accurate effective index difference between the LP_{01} mode and the LP_{11} mode, we can reproduce or prove the refractive index profile of the multiple-ring TMF. We both carry out the experiment and simulation to support this point in the following sections.

III. Results and Discussion

First, we captured the cross-section of the multiple-ring TMF by using optical microscope, which is shown in Fig. 2. Here, the radius of core is labeled as R1, the radius of the ring 1 and ring 2 are labeled as R2 and R3, respectively, and the radius of cladding is labeled as R4.

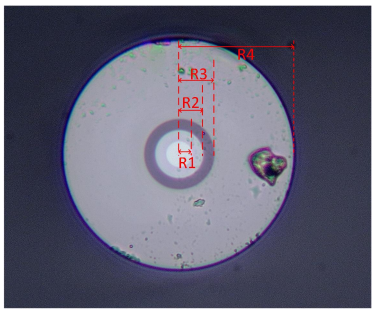

Fig. 2. The cross-section of the multiple-ring TMF captured by an optical microscope.

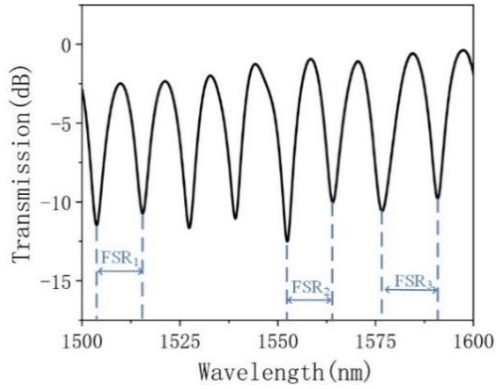

Fig. 3. Transmission spectrum generated by lateral-offset aligning a 35.4cm-length multiple-ring TMF with two SMFs.

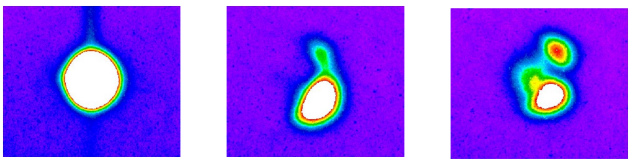

Fig. 4. Near field patterns captured by infrared CCD with the lateral-offset value increasing to confirm the modal interference of the LP_{01} mode and the LP_{11} mode.

This work was supported by the National Natural Science Foundation of China, under Project 62205067, 62005052.

We use a segment of the multiple-ring TMF with a length of 35.4 cm in the experimental study. We build an experimental setup to support the generation of modal interference fringes with the multiple-ring TMF, two SMFs, broadband light source, and optical spectrum analyzer (OSA). The measured transmission spectrum is shown in Fig. 3. The FSR increases when the resonant dip of the wavelength operates at the infrared area. Three FSRs are labeled in the figure, which are FSR_1, FSR_2 and FSR_3. The values of the FSR_1, FSR_2 and FSR_3 are about 11.81 nm, 13.12 nm, and 13.84 nm, respectively. Δn_{eff} is deduced to be about $5.792 \text{ X } 10^{-4}$ at the wavelength of 1558 nm.

To confirm the interference fringes is generated by the modal interference of the LP_{01} mode and the LP_{11} mode. Near filed pattern from the output end of the multiple-ring TMF is captured by an infrared CCD. As shown in Fig. 4, with the lateral-offset value increasing, the mode filed of the LP_{11} mode becomes clearer at the wavelength of the resonant dip.

To study the model of such kind of fiber, we use finite-element method (FEM)-based commercial software COMSOL to analyze the modal dispersion of the multiple-ring TMF. The initial parameters of the multiple-ring TMF are given in the follow, where the core radius (R1), the ring 1 radius (R2), the ring 2 radius(R3) and the cladding radius(R4) are about 7.0 μm , 13.0 μm , 19.0 μm and 62.5 μm , respectively, and the refractive index of core, ring 1, ring 2, and the cladding are 1.4485, 1.444, 1.435336 and 1.444, respectively. In the simulation, the modal dispersion curve is shown in Fig. 5(a), where the effective index difference of the LP_{01} mode and the LP_{11} mode is calculated to be about $1.99\ X\ 10^{-3}$ at the wavelength of 1550 nm, which is shown in Fig. 5(b). The simulation is far from the experimental one, and there should be some deviations among the fiber parameters above.

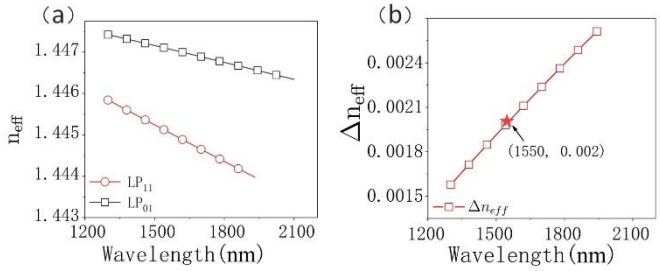

Fig. 5. (a) Effective indices of the LP_{01} mode and the LP_{11} mode against the wavelength; (b) the effective index difference of the LP_{01} mode and the LP_{11} mode.

To figure out which parameter that affect the modal dispersion of the multiple-ring TMF, we use elimination process to find out the key parameter of the fiber. In the fiber structure, we learn that the core radius and core refractive index, and the ring 1 radius and the ring 1 refractive index would be the key factors.

According to the provided fiber parameters, firstly, we fix other parameters of the multiple-ring TMF and only change the core refractive index. As shown in Fig. 6(a), the effective index of the LP_{01} mode and the LP_{11} mode increases with the core refractive index at the wavelength of 1550 nm. The increasing of the effective index of the LP_{01} mode is faster than the LP_{11} mode, which is shown in the

effective index difference of the LP_{01} mode and the LP_{11} mode in Fig. 6(b). Then we fix other parameters of the multiple-ring TMF and only change the core radius. As shown in Fig. 6(c), the effective index of the LP_{01} mode and the LP_{11} mode increases with the core radius at the wavelength of 1550 nm. However, the increasing of the effective index of the LP_{11} mode is faster than the LP_{01} mode, which is shown in the effective index difference of the LP_{01} mode and the LP_{11} mode in Fig. 6(d).

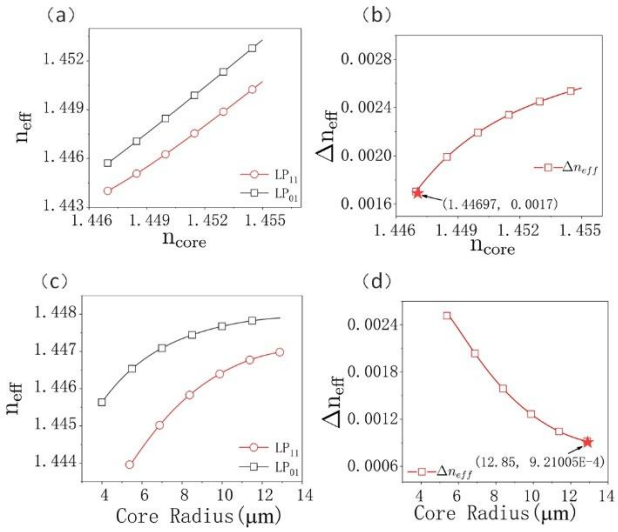

Fig. 6. (a) Effective indices of the LP_{01} mode and the LP_{11} mode against the core refractive index; (b) the effective index difference of the LP_{01} mode and the LP_{11} mode. (c) Effective indices of the LP_{01} mode and the LP_{11} mode against the core radius; (d) the effective index difference of the LP_{01} mode and the LP_{11} mode.

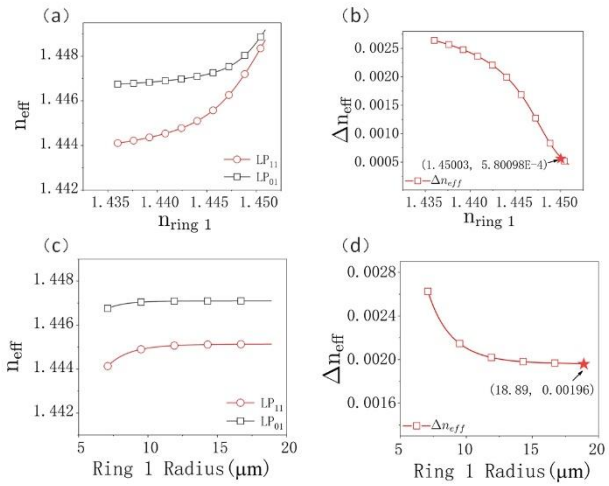

Fig. 7. (a) Effective indices of the LP_{01} mode and the LP_{11} mode against the ring 1 refractive index; (b) the effective index difference of the LP_{01} mode and the LP_{11} mode. (c) Effective indices of the LP_{01} mode and the LP_{11} mode against the ring 1 radius; (d) the effective index difference of the LP_{01} mode and the LP_{11} mode.

Later, we fix other parameters of the multiple-ring TMF and only change the ring 1 refractive index. As shown in Fig. 7(a), the effective index of the LP_{01} mode and the LP_{11} mode increases with the ring 1 refractive index at the wavelength of 1550 nm. However, the increasing of the effective index of the LP_{11} mode is faster than the LP_{01} mode, which is shown in the effective index difference of the LP_{01} mode and the LP_{11} mode in Fig. 7(b). Finally, we fix other parameters of the multiple-ring TMF and only change the ring 1 radius. As shown in Fig. 7(c), the effective index of the LP_{01} mode and the LP_{11} mode increases with the ring 1 radius at the wavelength of 1550 nm. However, the increasing of the effective index of the LP_{11} mode is faster than the LP_{01} mode, which is shown in the effective index difference of the LP_{01} mode and the LP_{11} mode in Fig. 7(d).

By systematically analyzing the fiber parameters variation characteristics, we select a group of fiber parameters that matches the trend of the experimental results. The combination of the parameters of the multiple-ring TMF are settled as follow. The core radius, the ring 1 radius, the ring 2 radius, and the cladding radius are about 8 μm, 16 μm, 21 μm and 62.5 μm, respectively, and the refractive index of core, ring 1, ring 2, and the cladding are 1.4485, 1.44867, 1.435336 and 1.444, respectively. In the simulation, the modal dispersion curve is shown in Fig. 8(a), where the effective index difference of the LP_{01} mode and the LP_{11} mode is calculated to be about $5.8044\,X\,10^{-4}$ at the wavelength of 1550 nm, which is shown in Fig. 8(b). The simulation results are well fitting with the experimental one.

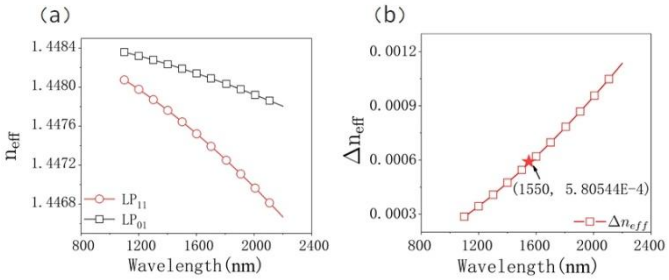

Fig. 8. (a) Effective indices of the LP_{01} mode and the LP_{11} mode against the wavelength; (b) the effective index difference of the LP_{01} mode and the LP_{11} mode.

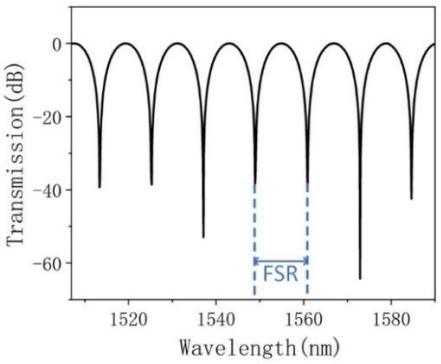

Fig. 9. Transmission spectrum generated by lateral-offset aligning a 35.4cm-length multiple-ring TMF with two SMFs in the simulation.

Finally, we simulate the transmission spectrum by using Eq. (1). As shown in Fig. 9, the transmission spectrum of the two-mode interference by the multiple-ring TMF length with a fiber length of 35.4 cm. The effective index difference of the LP_{01} mode and the LP_{11} mode is $5.753\,x\,10^{-4}$ at the wavelength of 1548nm with the FSR = 12 nm, which agrees with the experiment result of $5.792\,x\,10^{-4}$.

IV. Conclusion

We demonstrate a method to trace the refractive index profile of a multiple-ring TMF by using modal interference feedback, which can be extended to analyze all types of TMF

and FMF. The method is simple and easily to carry out, which can be developed as an algorithm in the fiber analysis system.

ACKNOWLEDGMENT

This work was supported by the National Natural Science Foundation of China, under Project 62205067, 62005052. The authors would like to thanks the undergraduate students (Mr. Q. Luo, Mr. H. Guo, Miss S. Jiang and Miss Y. Wu) to participate the extracurricular scientific research via this project.

REFERENCES

[1] B. J. Puttnam, G. Rademacher, and R. S. Luís, "Space-division multiplexing for optical fiber communications, " *Optica* vol. 8, no. 9, pp. 1186-1203, Sep. 2021.

[2] M. Olivero, A. Vallan, R. Orta and G. Perrone, "Single-Mode–Multimode–Single-Mode Optical Fiber Sensing Structure With Quasi-Two-Mode Fibers," *IEEE Transactions on Instrumentation and Measurement*, vol. 67, no. 5, pp. 1223-1229, May. 2018.

[3] P. Caramazza, O. Moran, and R. Murray-Smith, "Transmission of natural scene images through a multimode fibre," *Nature communications*, 10(1): 2029, May. 2019.

[4] E. S. Manuylovich, V. V. Dvoyrin, and S. K. Turitsyn, "Fast mode decomposition in few-mode fibers," *Nature communications*, 11(1): 5507, Nov. 2020.

[5] L. Zhang, J. Chen, E. Agrell, R. Lin and L. Wosinska, "Enabling Technologies for Optical Data Center Networks: Spatial Division Multiplexing," *J. Lightw. Technol.,* vol. 38, no. 1, pp. 18-30, Sep. 2019.

[6] Q. Huang, J. Zhang, L. Zhong, Z. Zheng, J. Li and O. Xu, "Three-dimensional mode multiplexer based on adiabatic-tapered waveguides formed vertical directional couplers over C+ L band and beyond, " *Opt. Lett*. 48, 1044-1047, Feb. 2023.

[7] Q. Huang, X. Wang, J. Dong, Z. Zheng, O. Xu, S. Fu, P. Di, J. Li and Y. Qin, "Ultra-broadband LP 11 mode converter with high purity based on long-period fiber grating and an integrated Y-junction," *Optics Express*, 30(8): 12751-12759, Mar. 2022.

[8] Q. Huang, and K.S. Chiang, "Polarization-insensitive ultra-broadband mode filter based on a 3D graphene structure buried in an optical waveguide.," *Optica*,7(7):744-745, Jul. 2020.

[9] L. Zhong, Q. Huang, J. Zhang, Z. Zheng, J. Li, and O. Xu, "Reconfigurable ultra-broadband mode converter based on a two-mode fiber with pressure-loaded phase-shifted long-period alloyed waveguide grating," *Optics Express*, 31(5): 8286-8295, Feb. 2023.